

Trajectory Analysis for Small Satellite Payload Recovery from Low Earth Orbit

Hyungwon Kim* and Frank K. Lu†

University of Texas at Arlington, Arlington, Texas 76019

and

Larry N. McNay‡

TEXSAR, Fort Worth, Texas 76116

The reentry trajectories of a 227 kg mass at 91.4 km altitude and a velocity of 7.31 km/s was analyzed with a modified three degree-of-freedom technique. An estimate of the stagnation point heating was also made. The mass deployed an inflatable, three element drag disk decelerator that was modeled as a single circular disk, trailing the payload, normal to the direction of flight. It was found that the downrange distance decreased and the time of flight increased with increased decelerator area. The stagnation-point heat transfer rates with a decelerator of sufficiently low ballistic coefficient (24 Pa, 0.5 lb/ft²) was 5 to 10 percent that a typical ballistic reentry vehicle with a ballistic coefficient of 100 lb/ft² (4.8 kPa). The study did not find that staged deployment of the decelerator disks provided any aerodynamic advantages, particularly in view of the anticipated complexities involved in deploying such a system. Finally, skip trajectories yielded slightly lower stagnation-point heat transfer than the non-lifting case. However, they may not be advantageous since the increased flight time would expose the decelerator to a longer period of heating.

Nomenclature

C_D	= drag coefficient
Kn	= Knudsen number
LEO	= Low earth orbit
\dot{q}_c	= heat transfer rate
R_N	= nose radius
S	= cross-sectional area of decelerator
U	= velocity
ρ	= density

Subscripts

<i>cont</i>	= continuum limit
<i>CO</i>	= circular orbit (7.9 km/s, 26 kft/s)
<i>fm</i>	= free molecular limit
<i>ref</i>	= reference
<i>SL</i>	= sea level
∞	= freestream

Introduction

THERE is recent interest in using lightweight inflatable decelerators for recovering small payloads, such as LEO satellites, planetary sample return vehicles, sub-orbital rockets and high-altitude scientific balloons, without the weight penalty associated with retro

rockets and heat shields or tiles. Additionally, some payloads may require a system to accommodate premature recovery, such as in abortive launches, improper orbital insertions and spacecraft operational failures on orbit.

The increased presence of manned space flight in LEO has also caused increasing concern over hazards posed by space orbital debris. Several concepts have been proposed for reducing the hazards that space orbital debris can pose both in LEO and on the ground. For example, space vehicles in LEO reaching the end of their mission life can be de-orbited or placed in a reduced lifetime orbit to reduce the possibility of an accidental collision. The latter approach can be performed with controlled reentry maneuvers using retro-rockets, which can re-orbit the vehicle to a lower altitude or cause it to reenter and burn up. However, the need to carry additional fuel to accomplish such maneuvers will diminish the space vehicle's mission. Further, studies have indicated that some of the more massive components of the vehicle may not burn up completely and can reach the Earth's surface at locations that are hard to predict.

Currently under development is an alternate approach to spacecraft recovery. This approach uses an inflatable decelerator system that allows for a precision recovery of the entire vehicle from orbit. The first part of this system involves a large, lightweight inflatable structure that is designed to function as a low mass-area drag brake at high altitude. The second part of this system is a computer-guided parafoil recovery device. The inflatable structure is deployed in LEO to cause an orbital velocity decrease through aerobraking. This decrease in orbital velocity results in a rapid orbital decay of the satellite, which in turn initiates atmospheric reentry. The inflated structure continues to

Copyright ©2001 by the American Institute of Aeronautics and Astronautics, Inc. All rights reserved.

*Research Associate, Mechanical and Aerospace Engineering Department. Member AIAA.

†Professor and Director, Aerodynamics Research Center, Mechanical and Aerospace Engineering Department. Associate Fellow AIAA.

‡Vice President, 6777 Camp Bowie Boulevard, Suite 331.

generate increased drag as the vehicle falls deeper into the atmosphere. A successfully designed drag device will allow the overall vehicle to achieve subsonic velocities well above the optimum parafoil deployment altitude. Once the desired velocity and altitude has been achieved, the inflated structure is released and the autonomous parafoil is deployed for a precision guided final recovery. This may also be the safest way to reduce space orbital debris.

For example, in the recent attempt of the Russian-German Inflatable Reentry and Descent Technology vehicle, the shield inflates from a 1 m (3.3 ft) compact package up to 12–16 m (39–53 ft) shortly before reentry and then, if it survives reentry, functions as a drag cone to glide the payload back to earth. The concept of using inflatable decelerators for recovering payloads from space was actually proposed in the late 1940s.¹ In early experiments, nylon parachutes were deployed at altitudes in excess of 180 km (600 kft). The parachutes were found to partially inflate and then collapse cyclically at high altitude, before becoming fully inflated at low altitude. The outer edge of the parachute canopy was found to be melted. This was attributed to the high heating rates associated the high free-fall velocity when the parachute collapsed. To prevent canopy collapse, an inflated ring to artificially inflate the canopy was used successfully.² Based on this successful experiment, it was thought that a sufficiently large, high drag device could be used to de-orbit a satellite. If sufficient deceleration occurred high in the atmosphere, this would significantly reduce aerodynamic heating. However, calculations indicated that the anticipated maximum reentry temperatures far exceed the melting point of nylon. This concept was abandoned in favor of ablative heat shields. All state-of-the-art recovery systems utilize ablative heat shields and high-speed parachutes, or heat tiles and winged vehicles for final recovery, all of which carry a severe weight penalty.

Only recently have advances in materials technology made the concept of high-altitude payload recovery feasible. Preliminary estimates indicate that an inflatable drag device with a low ballistic coefficient ($W/C_D S = 24 \text{ Pa}$ or 0.5 lb/ft^2) can operate within the maximum reentry temperatures of recent high-temperature inflatable materials. Such a concept has benefits such as reduced weight compared to ablative heat shields and tiles, lower g -loading on reentry, and the elimination of retro-rockets used for initiating orbital departure.

A concept is being developed where a large inflatable decelerator is deployed in LEO to recover a payload from space. This concept is shown schematically in Fig. 1. It consists of three inflatable drag plate decelerator disks that can be deployed in space.

The two basic methods of withstanding reentry heating are ablation shielding and radiative cooling. Reentry devices that incorporate low ballistic coefficients take advantage of radiation cooling during reentry. A radiative material can withstand high total heat loads as long as the maximum heating rate does not exceed the capability of the material. The permissible heating rate is a function of temperature, time at temperature of the material, emissivity of the material, and heat capacity of the material. Stagnation points on the reentry

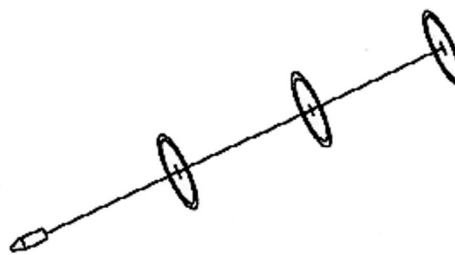


Figure 1: Schematic of payload recovery concept.

structure experience the highest heating rates. Stagnation points that have a large radius of curvature help to reduce local heating rates. If a reentry system is light enough (low mass-area ratio) that it can be decelerated to relatively low speeds, even if acted on by low drag forces, then the convective heating is minimized by employing shapes with high-pressure drag (blunt bodies with large radii of curvature). Such shapes maximize the amount of heat delivered to the atmosphere and minimize the amount of heat delivered to the drag device during deceleration.

The advantage of deploying a secondary drag body to achieve a low ballistic coefficient configuration is that it shifts a large portion of the total heat load (as much as 80 percent) away from the primary body. The main payload section (satellite, etc.) is able to make a relatively cool reentry. Little or no redesign would be needed for the payload due to the entire heat load being assumed by the add-on recovery device.

The concept of stacking several drag plates in series is seen as an effective solution to achieving the desired ballistic coefficient. A combination of two or more identical drag plates in series is additive with respect to drag coefficient.³ This condition holds true as long as the spacing between each disk is sufficient. The optimum spacing between drag plates in series is seven disk diameters.⁴ This optimum spacing allows the detached flow going around the first disk to reattach prior to encountering the second disk. The second disk can then generate the same maximum drag coefficient of $C_D = 1.2$ that the first disk generates. The two disks create a combined drag coefficient of $C_D = 2.4$ for the system. The addition of a third drag plate in series brings the combined total drag coefficient to $C_D = 3.6$ for the entire system.

Examination of a single, flat disk drag plate at hypersonic speeds found that the drag coefficient value remains constant at $C_D = 1.2$ for Reynolds numbers greater than 100. In addition, published data based on drag plate research shows that a two-disk configuration in series generates a drag coefficient twice that of a single disk ($C_D = 2.4$) for Reynolds numbers 102 and greater. One advantage of this tandem configuration is that each individual disk can be made smaller as opposed to using one single disk to meet the ballistic coefficient requirements. This provides a significant reduction in inflatable material surface area, and thus a proportional reduction in weight.

This paper reports on a preliminary analysis of the

trajectory when a small representative payload of 226.8 kg (500 lbm) is de-orbited from an altitude of 91.4 km (300 kft), where it is traveling at 7.31 km/s (24 kft/s). Different decelerator concepts were examined. The trajectories were compared with a typical Apollo capsule type reentry trajectory having a ballistic coefficient $W/(C_D S)$ of 4.8 kPa (100 lb/ft²). Skipping trajectories were also examined as part of this analysis.

Method

Trajectories of the reentry vehicle were computed using the Trajectory Simulation and Analysis Program TSAP.⁵ TSAP solves for point-mass trajectory problems. The code allows the body attitude to be defined and includes the ability to define aerodynamic and propulsion models of arbitrary complexity. During the reentry process, the aerodynamic parameters are first characterized by free molecular flow. The code then allows the simulation to follow a gradual transition to continuum flow as the satellite descends into the denser parts of the atmosphere. Thus, despite being a three degree-of-freedom model, TSAP can reliably simulate trajectories for any vehicle having predictable body dynamics. It has been used for many types of aerospace vehicles such as aircraft, rocket boosters, spacecraft and reentry vehicles. TSAP enables as many as 99 trajectory segments to be defined since a given mission profile might require a vehicle to assume several configurations and guidance strategies. For this study, TSAP was run on Sun workstations.

As part of the post-processing procedure, aerodynamic drag coefficients were obtained from a simple estimation function⁶ of the form:

$$C_D = \frac{Kn + 0.008}{Kn + 0.09} (C_{D,fm} - C_{D,cont}) + C_{D,cont}. \quad (1)$$

In Eq. (1), $C_{D,fm} = 4.0$ and $C_{D,cont} = 1.17$.

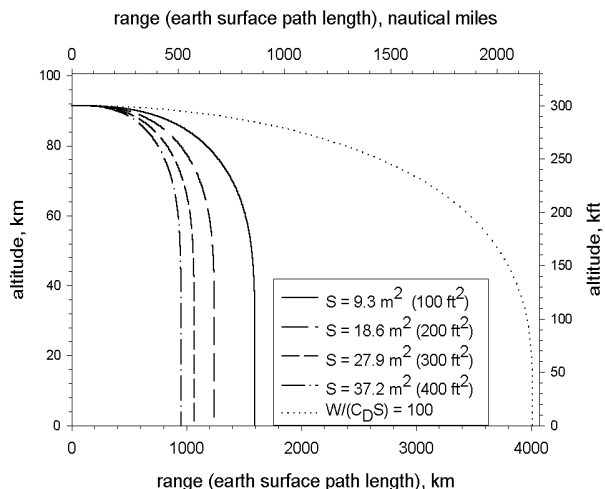
The convective heat transfer to the stagnation-point along trajectories of the reentry vehicle was calculated using^{7,8}

$$\dot{q}_c = \frac{17600}{R_N^{0.5}} \left(\frac{\rho_\infty}{\rho_{SL}} \right)^{0.5} \left(\frac{U_\infty}{U_{CO}} \right)^{3.15}. \quad (2)$$

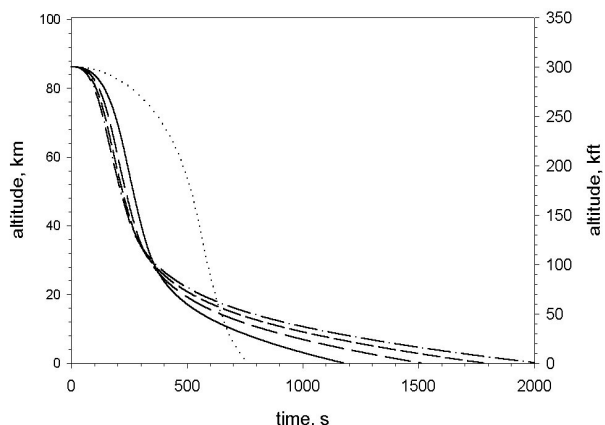
The effective nose radius for flat disk was estimated using^{8,9}

$$R_{N,eff} = 1.667 D_{flatdisk}. \quad (3)$$

Finally, high temperatures in high-speed atmospheric flight require that the properties behind a shock wave must be obtained using an equilibrium chemically reacting air model instead of a calorically perfect air model. The temperature and density ratios in the shock layer along some trajectory points were obtained from the results of Huber^{10,11} that give the variations of shock temperature and density with velocity and altitude. The equilibrium composition of air at the corresponding temperature and density of the shock layer was computed using the CEA code.¹²



a. Range



b. Time of descent

Figure 2: Trajectories of payload recovery vehicle with different disk areas.

Results

Single Disk

Some selected results are presented here for a 226.8 kg (500 lbm) vehicle at 91.4 km (300 kft) altitude, a velocity of 7.31 km/s (24 kft/s) and a flight path angle of zero deg. The calculations were done for a single disk with areas of $S_{ref} = 9.3, 18.6, 27.9, 37.2$ m² (100, 200, 300, 400 ft²). For the present preliminary analysis, a single disk was used to represent the multiple, tandem disks. The trajectory of a purely ballistic reentry vehicle with a ballistic coefficient $W/(C_D S) = 100$ was also computed for general comparison. The initial conditions for this vehicle were assumed the same as those of the payload recovery vehicle.

Figure 2 is a comparison of calculated trajectories for each disk while Fig. 3 shows the velocity-altitude maps and velocity histories. The disk with the largest area had the most aerodynamic drag and, therefore, the most severe initial deceleration (Fig. 3b). The large aerodynamic drag yielded the shortest downrange (Fig. 2a) but also the longest deorbit time (Fig. 2b).

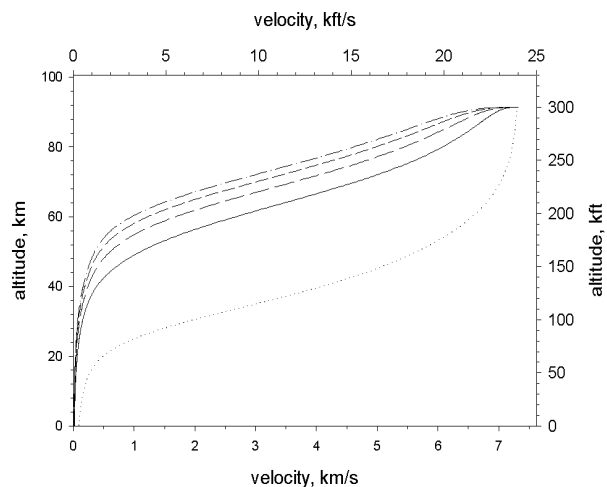
For the purely ballistic reentry case, the lack of aerodynamic drag yielded the longest downrange but also the shortest de-orbit time.

The gentler descent with decelerator disks is expected to yield lower convective heat transfer rates. This can be seen in Fig. 4. The most severe heating is encountered by the smallest disk. However, for all the four disks, the peak heating is far lower than the purely ballistic reentry case at about 5–10 percent of the latter. The peak heating condition occurs early in the trajectory, when the dynamic pressure is still low. Deploying inflatable aerodynamic decelerators in LEO is therefore beneficial from a heat transfer standpoint. However, this is also the moment of the most severe deceleration. This is clearly evident in a plot of the total g -loading (Fig. 5). Moreover, it can be seen that the g -loading for the four disks are of similar magnitude and their peaks are not significantly lower than the ballistic reentry case, being only about 10 percent lower than that the latter. The peak loading occurs during a time when the altitude decreases rapidly and the payload enters the lower atmosphere. One can conclude that the peak aerodynamic g -loading is not significantly affected by the use of inflatable decelerators.

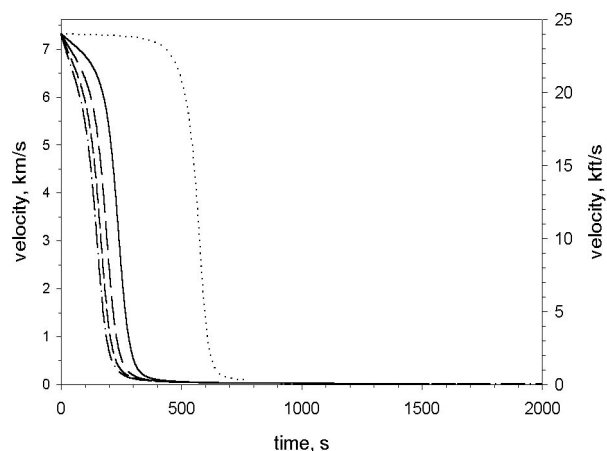
Staged Disk Deployment

Two cases where the disk area was abruptly increased, or staged, were also examined. This was done to simulate the different interactions of the drag plates in free molecular flow (found in LEO), and continuum flow encountered at lower transition altitudes. In free molecular flow, the first disk in the drag plate series is the only one generating any drag effect. However, the drag coefficient for a disk in free molecular flow ($C_D \approx 4.0$) is found to be much higher than a single disk in continuum flow. Once the drag plate configuration (three disks in series) reaches the continuum flow transition altitude, all three disks generate a combined drag coefficient of $C_D \approx 3.6$. The resulting ballistic coefficient remains essentially the same through the free molecular flow region and into the continuum flow region. The area change models ranged from 9.3 to 27.9 m² (100 to 300 ft²) and from 12.4 to 37.2 m² (133 to 400 ft²). The area change was assumed to occur instantly at the transition altitude. The transition altitudes were chosen as 68.6, 76.2 and 83.8 km (225, 250, 275 kft). The results are shown in Fig. 6–10 for the former scheme. Results for the latter scheme are qualitatively similar and are not presented for brevity.

The results indicate that the range, flight time or stagnation point heating are not much affected by the staged area increase at transition altitude compared to the constant area case. For example, Fig. 7 indicates a downrange of about 1,500 km for the three disk configuration of staged deployment at transition altitude, while the downrange for a disk of constant area of 9.3 m² (100 ft²) is about 1,600 km. Finally, the extremely large g -loading is an artifact due to the sudden deceleration specified in the simulation model. This result is thus meaningless since, in practice, any staged transition will develop more gently. There appears to be no adverse results when a multiple disk drag plate config-



a. Variation with altitude



b. Variation with time

Figure 3: Reentry velocities. (For legend, see Fig. 2.)

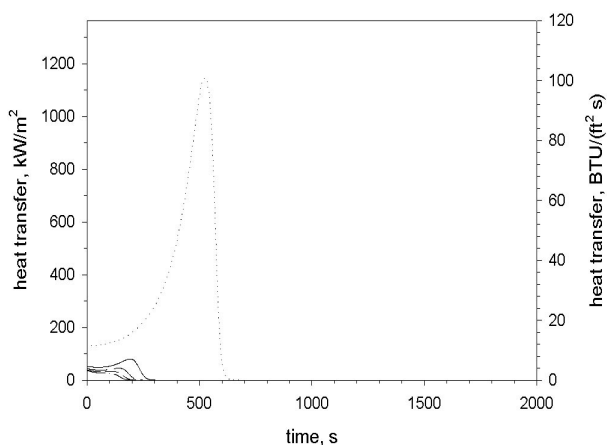


Figure 4: Convective heat transfer rates. (For legend, see Fig. 2.)

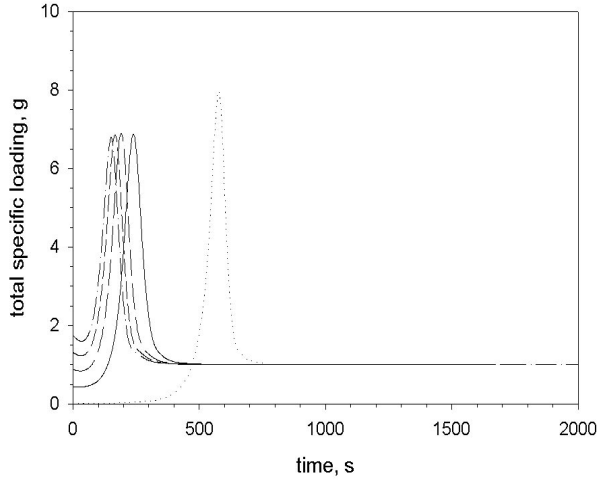


Figure 5: Total g -loadings. (For legend, see Fig. 2.)

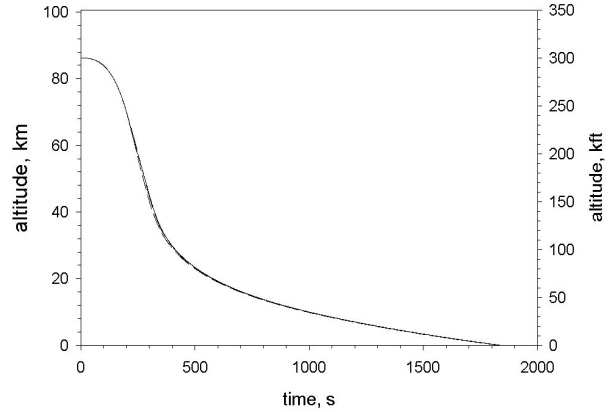


Figure 7: Trajectory for staged disk deployment, $S = 9.3 \rightarrow 18.6 \text{ m}^2$ ($100 \rightarrow 300 \text{ ft}^2$). (For legend, see Fig. 6.)

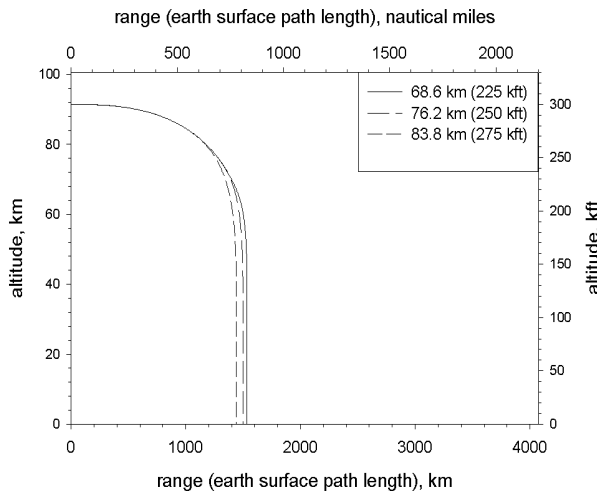


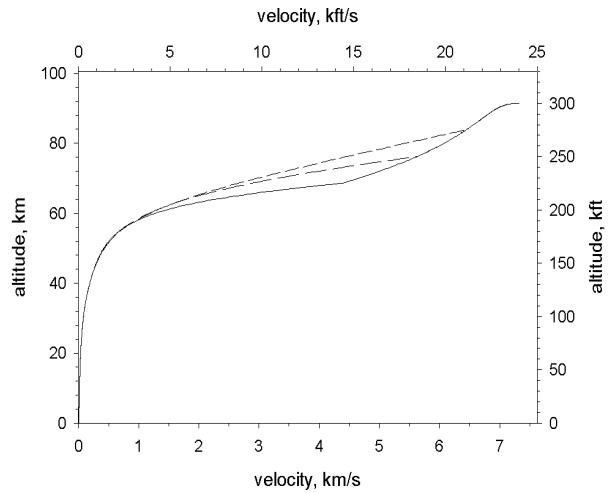
Figure 6: Range for staged disk deployment, $S = 9.3 \rightarrow 18.6 \text{ m}^2$ ($100 \rightarrow 300 \text{ ft}^2$).

uration is used versus a single large disk.

Effect of Lift

The possibility of skip pattern trajectories was examined with the introduction of lift forces. The calculations were performed with $C_L = 0, 0.5, 1.0$ for a disk of 9.3 m^2 (100 ft^2). It was thought that lift will result in a gentler trajectory, thus reducing peak heating and g -loading.

Figure 11 shows that lift significantly increases the downrange of the reentry trajectory. A proportionately larger share of the deceleration occurs at a higher altitude (Fig. 12a). This also results in a decrease in peak heating and g -loading compared to the non-lifting case. These results are shown in Figs. 14 and 15.



a. Variation with altitude

b. Variation with time

Figure 8: Reentry for staged disk deployment, $S = 9.3 \rightarrow 18.6 \text{ m}^2$ ($100 \rightarrow 300 \text{ ft}^2$). (For legend, see Fig. 6.)

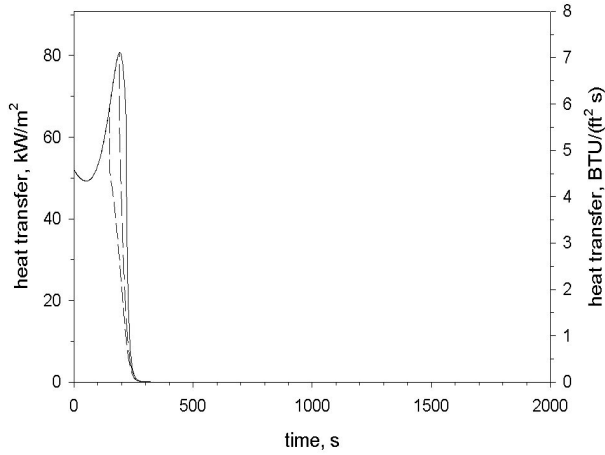


Figure 9: Stagnation point heating for staged disk deployment, $S = 9.3 \rightarrow 18.6 \text{ m}^2$ ($100 \rightarrow 300 \text{ ft}^2$). (For legend, see Fig. 6.)

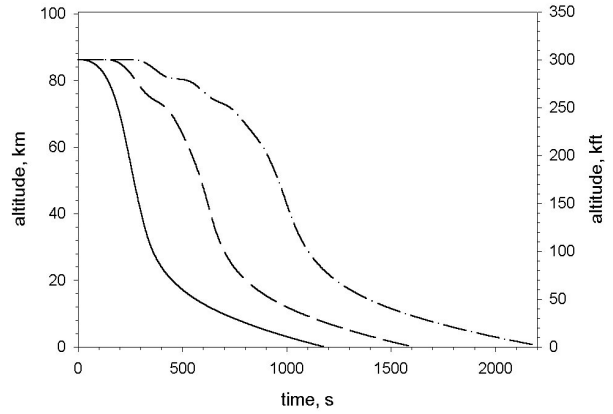


Figure 12: Trajectory (skip trajectory). (For legend, see Fig. 11.)

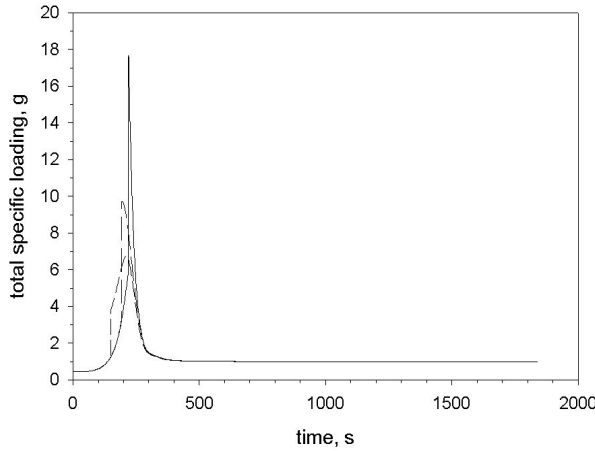
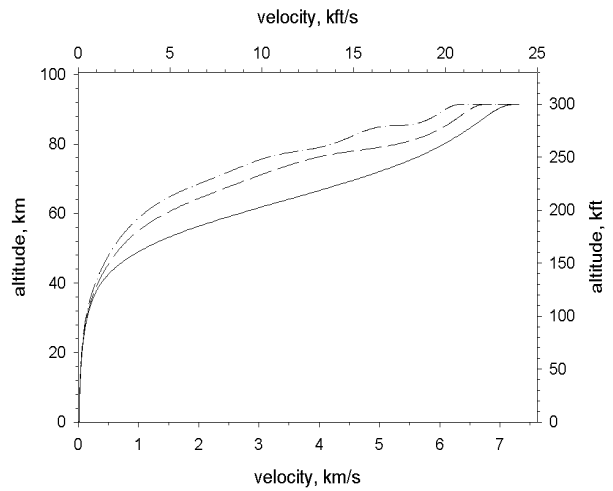


Figure 10: g -loading for staged disk deployment, $S = 9.3 \rightarrow 18.6 \text{ m}^2$ ($100 \rightarrow 300 \text{ ft}^2$). (For legend, see Fig. 6.)



a. Variation with altitude

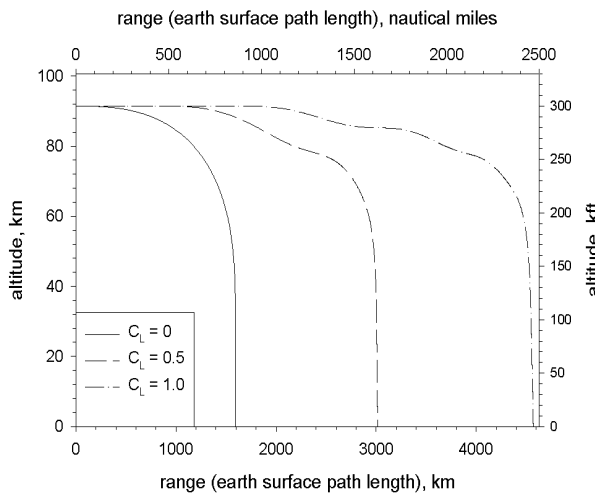
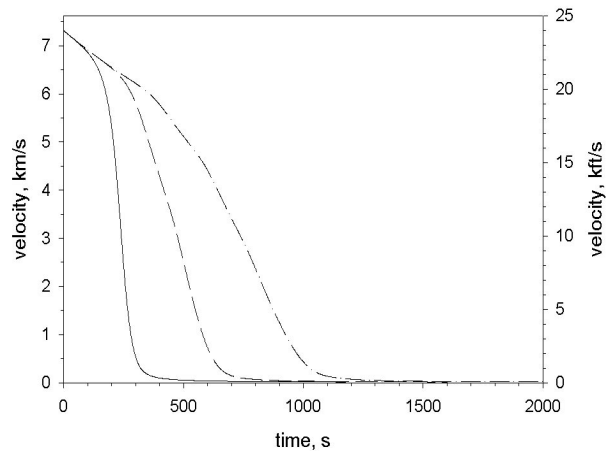


Figure 11: Range (skip trajectory).



b. Variation with time

Figure 13: Reentry (skip trajectory). (For legend, see Fig. 11.)

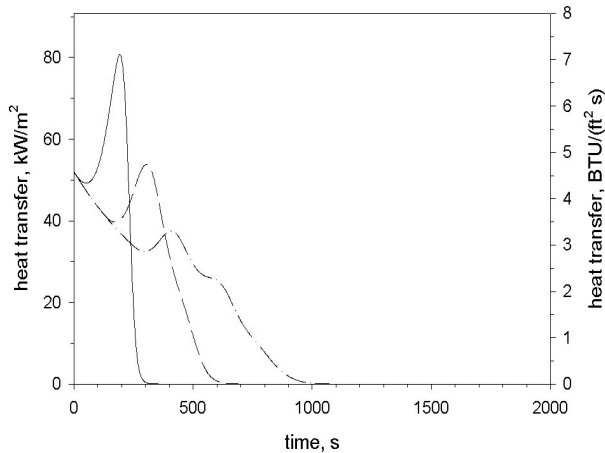


Figure 14: Stagnation point heating (skip trajectory). (For legend, see Fig. 11.)

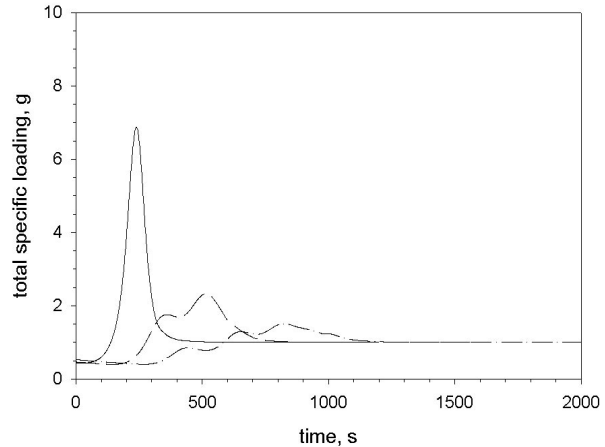


Figure 15: g -loading (skip trajectory). (For legend, see Fig. 11.)

Conclusions

An exploratory study was made of the reentry trajectories of a 227 kg mass at 91.4 km altitude and a velocity of 7.31 km/s with a modified three degree-of-freedom technique. The mass and decelerator were modeled as a single circular disk normal to the flight direction. The downrange decreased and the time of flight increased with decelerator area. The stagnation-point heat transfer rates with decelerators were 5 to 10 percent of that of a purely ballistic reentry vehicle having a ballistic coefficient of 4.8 kPa (100 lb/ft²), thus showing the advantage of deploying inflatable aerodynamic decelerators. The study did not find that the staged deployment of the decelerators transitioning from free molecular flow to continuum flow had any adverse results compared to a single large disk of constant area. Finally, skip trajectories yielded slightly lower stagnation-point heat transfer than the non-lifting case. But they may not be advantageous since the longer flight time would expose the decelerator to a longer period of heating.

Acknowledgements

This work was partly funded by the USAF Research laboratory, Kirtland AFB, New Mexico, under Contract F29601-98-C-0111. The authors gratefully acknowledge the assistance of Drs. Timothy Bartel and Mikhail Gallis of Sandia National Laboratories, Albuquerque, New Mexico, for making the TSAP code available.

References

- ¹Koelle, H. H., ed., *Handbook of Astronautical Engineering*, McGraw-Hill, New York, 1961.
- ²Knacke, T. W., Bixby, H. W., Ewing, E. G., "Recovery Systems Design Guide," AFFDL-TR-78-151, Air Force Fight Dynamics Laboratory, WPAFB, OH, December 1978.

³Hoerner, S. F., *Fluid-Dynamic Drag*, Hoerner Publishing, Midland Park, NJ, 1958.

⁴Berndt, R. J., DeWeese, J. H., "Drag Characteristics of Several Two-Body Systems at Transonic and Supersonic Speeds," RTD-TDR-63-4226, Air Force Fight Dynamics Laboratory, WPAFB, OH, December 1964.

⁵Outka, D. E., "User's Manual for the Trajectory Simulation and Analysis Program (TSAP)," SAND 88-3158, July 1990.

⁶Bartel, T. J., facsimile note to Larry McNay, Sandia National Laboratories, June 15, 1999.

⁷Detra, R. W., Kemp, N. H. and Riddel, F. R., "Addendum to Heat Transfer to Satellite Vehicles Reentering the Atmosphere," *Jet Propulsion*, Vol. 27, No. 12, pp. 1256-1257, December 1957.

⁸Bertin, J. J., *Hypersonic Aerothermodynamics*, AIAA Education Series, AIAA, 1994.

⁹Boison, J. C. and Curtiss, H. A., "An Experimental Investigation of Blunt Body Stagnation Point Velocity Gradient," *ARS Journal*, Vol. 29, No. 2, pp. 130-135, February 1959.

¹⁰Huber, P. W., "Hypersonic Shock-Heated Flow Parameters for Velocities to 46,000 Feet per Second and Altitudes to 323,000 Feet," NASA TR R-163, December 1963.

¹¹Anderson, J. D., *Hypersonic and High Temperature Gasdynamics*, McGraw-Hill, 1989.

¹²Gordon, S. and McBride, B. J., "Computer Program for Calculation of Complex Chemical Equilibrium Compositions and Applications - I. Analysis," NASA-RP-1311, October 1994.